



Cite this: *Phys. Chem. Chem. Phys.*,
2015, 17, 1025

Analytic gradients, geometry optimization and excited state potential energy surfaces from the particle-particle random phase approximation†

Du Zhang,^a Degao Peng,^a Peng Zhang^a and Weitao Yang^{*ab}

The energy gradient for electronic excited states is of immense interest not only for spectroscopy but also for the theoretical study of photochemical reactions. We present the analytic excited state energy gradient of the particle-particle random phase approximation (pp-RPA). The analytic gradient formula is developed from an approach similar to that of time-dependent density-functional theory (TDDFT). The formula is verified for both the Hartree–Fock and (Generalized) Kohn–Sham reference states *via* comparison with finite difference results. The excited state potential energy surfaces and optimized geometries of some small molecules are investigated, yielding results of similar or better quality compared to adiabatic TDDFT. The singlet-to-triplet instability in TDDFT resulting in underestimated energies of the lowest triplet states is eliminated by pp-RPA. Charge transfer excitations and double excitations, which are challenging for most adiabatic TDDFT methods, can be reasonably well captured by pp-RPA. Within this framework, ground state potential energy surfaces of stretched single bonds can also be described well.

Received 12th September 2014,
Accepted 3rd November 2014

DOI: 10.1039/c4cp04109g

www.rsc.org/pccp

1. Introduction

The theoretical description of electronic excitation energies and excited state potential energy surfaces is of great significance in chemistry, biology, materials science, *etc.* It provides insight into highly relevant topics such as artificial photosynthesis and design of solar cells.^{1–3} The development of electronic structure theories based on quantum mechanics has thus enabled the mechanistic understanding of electronic excitations. There are several categories of electronic structure theories for describing excited states. The first category uses the many-body wave function as the basic variable. The simplest of this category is configuration interaction singles (CIS)⁴ and its perturbative corrections like CIS(D).^{5,6} Higher level methods include multi-reference coupled-cluster theories (MRCC),⁷ complete active space second order perturbation theory (CASPT2),^{8–11} and equation-of-motion and linear response coupled-cluster theories (EOM-CC and LR-CC),^{12–15} which are generally of higher accuracy but are also more computationally demanding. The second category is based on the density functional theory (DFT)^{16–18} formulation of quantum mechanics, and in particular time-dependent density

functional theory (TDDFT) within the adiabatic approximation^{19–21} has been extensively applied to both finite and extended systems. The third category of methods is developed from the Green's function approach, of which the *GW*-Bethe–Salpeter equation (*GW*-BSE) method within the static approximation has become a standard way of treating solids.^{22–26} Recent extension of the BSE beyond the static approximation²⁷ has shown very promising results. Highly accurate results have been obtained for atomic and molecular systems even with a second-order dynamical Bethe–Salpeter kernel,²⁸ which also provides a unique perspective of the connection to TDDFT beyond the adiabatic approximation.^{29–31} The construction of a frequency-dependent two-point TDDFT kernel from the static four-point BSE kernel by Gatti *et al.* illustrates the trading of spatial non-locality and time-nonlocality between BSE and TDDFT, furthering the understanding of the frequency-dependent nature of the TDDFT kernel.³² In addition, methods based on the particle-particle channel two-particle Green's function serve as yet another approach.^{33,34} With the particle-particle random phase approximation (pp-RPA), superior results of Rydberg, double and charge transfer excitations compared to adiabatic TDDFT have already been obtained.³⁴ Moreover, the pp-RPA has recently been used to obtain correlation energy for chemical systems by virtue of the adiabatic-connection fluctuation-dissipation theorem (AC-FDT).³⁵ It is the first density functional approximation (DFA) to satisfy the flat-plane conditions,³⁶ outperforming the traditional particle-hole RPA (ph-RPA) in many ways.³⁷ Theoretical analysis has also established the equivalence between pp-RPA and ladder coupled-cluster

^a Department of Chemistry, Duke University, Durham, NC 27708, USA.

E-mail: weitao.yang@duke.edu

^b Key Laboratory of Theoretical Chemistry of Environment, School of Chemistry and Environment, South China Normal University, Guangzhou 510006, China

† Electronic supplementary information (ESI) available. See DOI: 10.1039/c4cp04109g

doubles (I-CCD),^{38,39} making an interesting connection between orbital dependent DFAs and *ab initio* wave-function-based quantum chemistry methods.

In addition to obtaining vertical excitation energies, it would be important to explore excited state total energy gradients and potential energy surfaces in order to understand photochemical processes. The cornerstone of most electronic structure theory tools for ground state and excited state gradients and other response properties is the coupled-perturbed self-consistent field (CPSCF) equation,⁴⁰ which yield the first derivatives of molecular orbital coefficient relaxation. The excited state analytic energy gradient is obtained by adding up the analytic ground state energy gradient and the analytic excitation energy gradient. The analytic gradient equations have been developed and extensively implemented for excited state theories like CIS,⁴ TDDFT^{41–44} as well as other higher-level theories.^{45–47} Such developments make excited state geometry optimization and MD simulations possible,⁴⁸ expanding the scope of electronic structure theory into the realm of complex chemical processes involving excited states. In this work, the development of a pp-RPA analytic excited state energy gradient proceeds in a manner similar to the TDDFT analytic gradient. The total energy gradient is the sum of the ground state and the excitation energy gradients.

II. Theoretical development

II. 1. The pp-RPA equation and its extension to non-canonical molecular orbital basis

In this section we review the pp-RPA equation and its extension to the non-canonical molecular orbital basis.

The pp-RPA generalized eigenvalue equation can be solved to obtain the double-electron-addition energies,³⁵

$$\begin{pmatrix} \mathbf{A} & \mathbf{B} \\ \mathbf{B}^\dagger & \mathbf{C} \end{pmatrix} \begin{pmatrix} \mathbf{X}^{n,N+2} \\ \mathbf{Y}^{n,N+2} \end{pmatrix} = \omega_n^{N+2} \begin{pmatrix} \mathbf{1} & \mathbf{0} \\ \mathbf{0} & -\mathbf{1} \end{pmatrix} \begin{pmatrix} \mathbf{X}^{n,N+2} \\ \mathbf{Y}^{n,N+2} \end{pmatrix}, \quad (1)$$

where

$$A_{ab,cd} = \delta_{ac}\delta_{bd}(\varepsilon_a + \varepsilon_b) + \frac{1}{2}[(ac|bd) - (ad|bc)], \quad (2)$$

$$B_{ab,ij} = \frac{1}{2}[(ai|bj) - (aj|bi)], \quad (3)$$

$$C_{ij,kl} = -\delta_{ik}\delta_{jl}(\varepsilon_i + \varepsilon_j) + \frac{1}{2}[(ik|jl) - (il|jk)], \quad (4)$$

$$X_{ab}^{n,N+2} = \langle \Psi_0^N | \hat{a}_a \hat{a}_b | \Psi_n^{N+2} \rangle, \quad (5)$$

$$Y_{ij}^{n,N+2} = \langle \Psi_0^N | \hat{a}_i \hat{a}_j | \Psi_n^{N+2} \rangle. \quad (6)$$

The indices a, b, c, d... stand for virtual orbitals, and i, j, k, l... stand for occupied orbitals. The orbital energies are denoted by ε_a , ε_b , etc. The two-electron integrals in the chemist's notation are (ac|bd), (ad|bc), etc. $|\Psi_0^N\rangle$ and $|\Psi_n^{N+2}\rangle$ stand for the N -particle ground state and the n th state (the ground state or an excited state) of the $(N+2)$ -particle system,

respectively. \hat{a}_a is the electron removal operator for orbital a. The eigenvalue ω_n^{N+2} stands for the double-electron-addition energy from $|\Psi_0^N\rangle$ to $|\Psi_n^{N+2}\rangle$. The eigenvectors for this set of solutions satisfy the normalization conditions

$$\langle X^{n,N+2}, Y^{n,N+2} | \Delta | X^{n,N+2}, Y^{n,N+2} \rangle = (\mathbf{X}^{n,N+2})^\dagger \mathbf{X}^{n,N+2} - (\mathbf{Y}^{n,N+2})^\dagger \mathbf{Y}^{n,N+2} = 1, \quad (7)$$

where

$$|X^{n,N+2}, Y^{n,N+2}\rangle = \begin{pmatrix} \mathbf{X}^{n,N+2} \\ \mathbf{Y}^{n,N+2} \end{pmatrix}, \quad (8)$$

$$\Delta = \begin{pmatrix} \mathbf{1} & \mathbf{0} \\ \mathbf{0} & -\mathbf{1} \end{pmatrix}. \quad (9)$$

Notice that the pp-RPA eqn (1) can be derived from the linear response of a molecular system in the presence of an external pairing field,⁴⁹ related to the formalism of DFT for superconductors⁵⁰ where both the normal density $\rho(\mathbf{x})$ and the anomalous/pairing density $\kappa(\mathbf{x},\mathbf{x}')$ are used as basic variables. By neglecting the many-body effects as contained in the exchange-correlation functional $E_{xc}[\rho,\kappa]$, the pp-RPA matrix elements do not contain the second derivative $g_{xc} = \frac{\delta^2 E_{xc}}{\delta\kappa^* \delta\kappa}$ except the ERIs resulting from the anomalous Hartree contribution. Nor does the derivative $f_{xc} = \frac{\delta^2 E_{xc}}{\delta\rho \delta\rho}$ come in here because of the absence of a particle-hole perturbation that couples to $\delta\rho$, which is present in the conventional particle-hole TDDFT.

The same matrix eqn (1) has another set of solutions that correspond to double-electron-removal energies ω_n^{N-2} . The eigenvalue ω_n^{N-2} stands for the double-electron-removal energy from $|\Psi_0^N\rangle$ to $|\Psi_n^{N-2}\rangle$, for which the eigenvectors are given by

$$X_{ab}^{n,N-2} = \langle \Psi_0^N | \hat{a}_a \hat{a}_b | \Psi_n^{N-2} \rangle, \quad (10)$$

$$Y_{ij}^{n,N-2} = \langle \Psi_0^N | \hat{a}_i \hat{a}_j | \Psi_n^{N-2} \rangle, \quad (11)$$

which satisfy the following normalization conditions

$$\langle X^{n,N-2}, Y^{n,N-2} | \Delta | X^{n,N-2}, Y^{n,N-2} \rangle = -1. \quad (12)$$

As an extension, if we use orthonormal molecular orbitals that are unitarily transformed from the canonical orbitals, the matrix elements become

$$A_{ab,cd} = \delta_{ac}\langle b|H_s|d\rangle + \delta_{bd}\langle a|H_s|c\rangle + \frac{1}{2}[(ac|bd) - (ad|bc)], \quad (13)$$

$$B_{ab,ij} = \frac{1}{2}[(ai|bj) - (aj|bi)], \quad (14)$$

$$C_{ij,kl} = -\delta_{ik}\langle j|H_s|l\rangle - \delta_{jl}\langle i|H_s|k\rangle + \frac{1}{2}[(ik|jl) - (il|jk)]. \quad (15)$$

where H_s is the HF or DFT effective one-electron operator defined as

$$H_s = -\frac{1}{2}\nabla_{\mathbf{r}}^2 + v(\mathbf{r}) + \int d\mathbf{x}' \frac{\rho(\mathbf{x}')}{|\mathbf{r} - \mathbf{r}'|} + v_{xc}(\mathbf{x}, \mathbf{x}') \\ = H^{\text{core}}(\mathbf{r}) + \int d\mathbf{x}' \frac{\rho(\mathbf{x}')}{|\mathbf{r} - \mathbf{r}'|} + v_{xc}(\mathbf{x}, \mathbf{x}'), \quad (16)$$

where in the second line we define the core Hamiltonian H^{core} . Here we allow the exchange–correlation potential to be non-local, which accounts for the case of the generalized Kohn–Sham theory, where v_{xc} can include both the local contribution from LDA/GGA and the non-local hybrid or long-range Hartree–Fock exchange contribution. Utilizing the antisymmetry of the eigenvectors

$$X_{ab}^n = -X_{ba}^n, \quad (17)$$

$$Y_{ij}^n = -Y_{ji}^n, \quad (18)$$

we can impose the restriction $i < j$, $a < b$ for eqn (1). Now the matrix elements of (1) become

$$A_{ab,cd} = \delta_{ac}\langle b|H_s|d\rangle + \delta_{bd}\langle a|H_s|c\rangle - \delta_{ad}\langle b|H_s|c\rangle - \delta_{bc}\langle a|H_s|d\rangle \\ + [(ac|bd) - (ad|bc)], \quad (19)$$

$$B_{ab,ij} = [(ai|bj) - (aj|bi)], \quad (20)$$

$$C_{ij,kl} = -\delta_{ik}\langle j|H_s|l\rangle - \delta_{jl}\langle i|H_s|k\rangle + \delta_{il}\langle j|H_s|k\rangle + \delta_{jk}\langle i|H_s|l\rangle \\ + [(ik|jl) - (il|jk)]. \quad (21)$$

Notice that with the restriction $i < j$, $a < b$, the terms $-\delta_{ad}\langle b|H_s|c\rangle - \delta_{bc}\langle a|H_s|d\rangle$ in (19) and $\delta_{il}\langle j|H_s|k\rangle + \delta_{jk}\langle i|H_s|l\rangle$ in (21) will drop out when using canonical orbitals, recovering eqn (12) of the supporting information of³⁵

$$A_{ab,cd} = \delta_{ac}\delta_{bd}(\epsilon_a + \epsilon_b) + [(ac|bd) - (ad|bc)], \quad (22)$$

$$B_{ab,ij} = [(ai|bj) - (aj|bi)], \quad (23)$$

$$C_{ij,kl} = -\delta_{ik}\delta_{jl}(\epsilon_i + \epsilon_j) + [(ik|jl) - (il|jk)]. \quad (24)$$

Eqn (19) to (21) will be useful for the development of the analytic excitation energy gradient.

II. 2. Calculation of the N -electron ground state and excited state energies from the $(N - 2)$ -electron reference system

According to Section II. 1., a calculation performed for the N -electron system gives information about the ground state and excited state energies of the $(N + 2)$ - and $(N - 2)$ -electron system,

$$E_n^{N-2} \leftarrow N \rightarrow E_n^{N+2}. \quad (25)$$

Therefore, to obtain the ground and excited state energies of the N -electron system, one can choose the $(N - 2)$ -electron system as reference as developed by Yang,³⁴

$$E_n^{N-4} \leftarrow N - 2 \rightarrow E_n^N. \quad (26)$$

The $(N + 2)$ -electron system in principle can also be used as reference but not in usual practice since the SCF $N + 2$ can often

be unbound. The N -electron ground state or excited state total energy of the system can be obtained *via*

$$E_n^N(\mathbf{A}) = E_0^{N-2}(\text{SCF}) + \omega_n^N, \quad (27)$$

where $E_0^{N-2}(\text{SCF})$ is the ground state SCF energy for the $(N - 2)$ -particle system and ω_n^N is the pp-RPA eigenvalue corresponding to the double-electron-addition excitation energy on top of the $(N - 2)$ -particle system. We shall denote this scheme as Plan A throughout the article. We note that this idea of calculating the ground state and excited state energies of the N -particle by resorting to another reference than the N -particle ground state had also been adopted in the spin-flip (SF)-TDDFT,^{51–54} where the lowest energy N -particle state of a higher spin is taken as reference on top of which a particle-hole excitation takes place. By taking the $(N - 2)$ -particle reference, pp-RPA, like SF-TDDFT, gives the qualitatively correct picture for systems with singlet-to-triplet instability and low-lying double excitations, later to be illustrated numerically.

Another scheme of calculating the total energy is given by

$$E_n^N(\mathbf{B}) = E_0^N(\text{SCF}) + (\omega_n^N - \omega_0^N), \quad (28)$$

where the total energy of the n th state for the N -particle system is calculated as the sum of the N -particle ground state SCF energy $E_0^N(\text{SCF})$ plus a difference in the double-electron-addition energies $(\omega_n^N - \omega_0^N)$. This scheme is denoted as Plan B. Notice that both plans give identical vertical excitation energies $(\omega_n^N - \omega_0^N)$ for the N -particle systems. They differ only in the way the N -particle ground state energy is calculated. Specifically, in Plan A (27) both the ground state and the excited states for the N -electron system can be viewed as double-electron-addition excited states from the SCF $(N - 2)$ -electron system, and thus the N -electron ground and excited states are treated on the same footing. This method can be viewed as a single-reference counterpart of the DIP/DEA-EOM-CC methods which use coupled-cluster references.^{55–57} The use of DFT reference within the pp-RPA connects to TDDFT-P, the time-dependent DFT in the pairing field with the neglect of the exchange-correlation kernel dependence on the pairing matrix.⁵⁸

At this point, we would like to specifically emphasize that for $n = 0$, eqn (27) yields the ground state energy for the N -particle system, which can alternatively be written as

$$E_0^N = E_0^{N-2} + \omega_0^N \\ = \min_{\langle \phi_i^{N-2} | \phi_j^{N-2} \rangle = \delta_{ij}} E_v^{N-2} [\{ \phi_i^{N-2} \}] \\ + \omega_0^N [\{ \phi_i^{N-2} \}]_{\text{minimizing } E_v^{N-2}, \mathbf{X}^{0,N}, \mathbf{Y}^{0,N}}. \quad (29)$$

The first term, the $N - 2$ SCF energy, is a functional of the KS/GKS orbitals for the $N - 2$ system, which are not necessarily the canonical ones (notice that even in the case of canonical orbitals, the $N - 2$ system's KS/GKS orbital energies are also functionals of the corresponding KS/GKS orbitals once the effective one-particle operator \hat{H}_s is given). The second term, the excitation energy ω_0^N , is a functional of the $N - 2$ KS/GKS orbitals and the pp-RPA vectors $\mathbf{X}^{0,N}$ and $\mathbf{Y}^{0,N}$. Notice that this

expression also indicates an uncoupled two-step calculation, where the orbitals in the second term ω_0^N are minimizers of the first term E_v^{N-2} . Now by virtue of the variational-principle definition of the eigenvectors $\mathbf{X}^{0,N}$ and $\mathbf{Y}^{0,N}$ corresponding to the lowest double electron addition energy, we have the following relation,

$$\begin{aligned}\omega_0^N &= \min_{\langle X, Y | A | X, Y \rangle = 1} \omega_v^N \left[\{ \phi_i^{N-2} \} \right]_{\text{minimizing } E_v^{N-2}, \mathbf{X}, \mathbf{Y}} \\ &= \min_{\langle X, Y | A | X, Y \rangle = 1} (\mathbf{X}^\dagger \quad \mathbf{Y}^\dagger) \begin{pmatrix} \mathbf{A} & \mathbf{B} \\ \mathbf{B}^\dagger & \mathbf{C} \end{pmatrix} \begin{pmatrix} \mathbf{X} \\ \mathbf{Y} \end{pmatrix} \Big|_{\{ \phi_i^{N-2} \} \text{ minimizing } E_v^{N-2}}\end{aligned}\quad (30)$$

where we used the normalization relation for the eigenvectors corresponding to double electron addition

$$\langle X^{n,N}, Y^{n,N} | A | X^{n,N}, Y^{n,N} \rangle = (\mathbf{X}^{n,N})^\dagger \mathbf{X}^{n,N} - (\mathbf{Y}^{n,N})^\dagger \mathbf{Y}^{n,N} = 1. \quad (31)$$

To summarize, the ground state total energy expression for the N -particle system is written as

$$\begin{aligned}E_0^N &= E_0^{N-2} + \omega_0^N \\ &= \min_{\langle \phi_i^{N-2} | \phi_j^{N-2} \rangle = \delta_{ij}} E_v^{N-2} [\{ \phi_i^{N-2} \}] \\ &\quad + \min_{\langle X, Y | A | X, Y \rangle = 1} \omega_v^N \left[\{ \phi_i^{N-2} \} \right]_{\text{minimizing } E_v^{N-2}, \mathbf{X}, \mathbf{Y}}.\end{aligned}\quad (32)$$

This expression defined a new pathway to calculate the ground state energy, which is very different from the normal orbital-dependent density functional for the ground state energy, like ph-RPA and pp-RPA. It follows a stepwise minimizing scheme. More interestingly, this new functional treats the exchange-correlation effect for the $N - 2$ system with traditional KS/GKS DFT (as in the E_0^{N-2} term) while also explicitly correlating the two electrons from the HOMO in a configuration-interaction-like manner (as in the ω_0^N term), thus combining the implicit treatment of the exchange-correlation effect by KS/GKS DFT and the explicit treatment of the correlation of the HOMO electrons. It is also physically well-grounded as viewed from a pairing field perturbation perspective.⁵⁸ Because it only uses the lowest excitation energy, the computational cost of this approach in eqn (32) is significantly lower than the pp-RPA correlation energy approach,³⁵ which uses all the excitation energies. Therefore, it opens up new opportunities in which the strengths of DFT and wave function methods may be seamlessly combined.

Finally, starting from eqn (30), we can obtain the first excited state energy in the following manner

$$\begin{aligned}E_1^N &= \min_{\langle \phi_i^{N-2} | \phi_j^{N-2} \rangle = \delta_{ij}} E_v^{N-2} [\{ \phi_i^{N-2} \}] \\ &\quad + \min_{\langle X, Y | A | X, Y \rangle = 1, \langle X, Y | A | X^{0,N}, Y^{0,N} \rangle = 0} \left(\omega_v^N \left[\{ \phi_i^{N-2} \} \right]_{\text{minimizing } E_v^{N-2}, \mathbf{X}, \mathbf{Y}} \right).\end{aligned}\quad (33)$$

Likewise, to obtain higher excited state energies, we only add extra orthogonality constraints to previous ones such that

the new variational space is orthogonal to the space spanned by the eigenvectors corresponding to states with lower energies. Thus the extension to excited states is successfully accomplished within this variational-principle picture.

II. 3. Analytic excitation energy gradient for pp-RPA

Starting from the matrix eqn (1) with the matrix elements given by (19) to (21), and by virtue of the Hellmann–Feynman theorem, the excitation energy gradient is calculated from

$$\frac{\partial \omega_n}{\partial \lambda} = (\mathbf{X}^n)^\dagger (\mathbf{Y}^n)^\dagger \left[\frac{\partial}{\partial \lambda} \begin{pmatrix} \mathbf{A}(\lambda) & \mathbf{B}(\lambda) \\ \mathbf{B}^\dagger(\lambda) & \mathbf{C}(\lambda) \end{pmatrix} \Big|_{\lambda=0} \right] \begin{pmatrix} \mathbf{X}^n \\ \mathbf{Y}^n \end{pmatrix}, \quad (34)$$

where the normalization is taken as

$$\langle X^n, Y^n | A | X^n, Y^n \rangle = (\mathbf{X}^n)^\dagger \mathbf{X}^n - (\mathbf{Y}^n)^\dagger \mathbf{Y}^n = 1 \quad (35)$$

for the double electron addition case. Also the matrices $\mathbf{A}(\lambda)$, $\mathbf{B}(\lambda)$ and $\mathbf{C}(\lambda)$ are constructed in terms of non-canonical perturbed orbitals, and the matrix elements are given by (19) to (21). The first derivative matrix elements $\frac{\partial}{\partial \lambda} A_{ab,cd}(\lambda)$, $\frac{\partial}{\partial \lambda} B_{ab,hi}(\lambda)$ and $\frac{\partial}{\partial \lambda} C_{ij,kl}(\lambda)$ have both direct contributions due to the nuclear coordinate shift of basis functions and indirect contributions due to the molecular orbital coefficient relaxation, which can be obtained by solving the CPSCF equations,⁴⁰

$$\mathbf{H}^{(1)} \mathbf{u}^\lambda = \mathbf{b}^\lambda, \quad (36)$$

where

$$H_{ai,bj}^{(1)} = \delta_{ab} \delta_{ij} (\varepsilon_a - \varepsilon_i) + \sum_{bj} [2(ai|bj) + 2(ai|f_{xc}|bj)], \quad (37)$$

$$\begin{aligned}b_{ai}^\lambda &= - \left\{ \frac{\partial}{\partial \lambda} \langle a | H^{\text{core}} | i \rangle + \frac{\partial}{\partial \lambda} \sum_j (ai|jj) + \sum_j \left(ai | f_{xc} | \frac{\partial}{\partial \lambda} jj \right) \right. \\ &\quad \left. + \left[\left\langle \frac{\partial}{\partial \lambda} a | v_{xc} | i \right\rangle + \left\langle a | v_{xc} | \frac{\partial}{\partial \lambda} i \right\rangle \right] \right\} \\ &\quad + \sum_{jk} O_{jk}^\lambda [(ai|jk) + (ai|f_{xc}|jk)] + \varepsilon_i O_{ai}^\lambda,\end{aligned}\quad (38)$$

where $\frac{\partial}{\partial \lambda}$ refers to the explicit derivative with respect to the spatial shift of nuclei positions in the Hamiltonian or the atomic orbitals, and $H^{\text{core}} = -\frac{1}{2} \nabla_{\mathbf{r}}^2 + v(\mathbf{r})$ is the core Hamiltonian. Also the matrix elements are given by

$$\langle a | H^{\text{core}} | i \rangle = \int d\mathbf{x} \phi_a^*(x) \left[-\frac{1}{2} \nabla_{\mathbf{r}}^2 + v_{\text{ext}}(\mathbf{r}) \right] \phi_i(\mathbf{x}), \quad (39)$$

$$(ai|bj) = \int d\mathbf{x}_1 \int d\mathbf{x}_2 \phi_a^*(\mathbf{x}_1) \phi_i(\mathbf{x}_1) \frac{1}{r_{12}} \phi_b(\mathbf{x}_2) \phi_j^*(\mathbf{x}_2), \quad (40)$$

$$\begin{aligned}(ai|f_{xc}|bj) &= \int d\mathbf{x}_1 \int d\mathbf{x}_1' \int d\mathbf{x}_2 \int d\mathbf{x}_2' \phi_a^*(\mathbf{x}_1) \phi_i(\mathbf{x}_1') \\ &\quad \times \frac{\delta^2 E_{xc}}{\delta \rho_s(\mathbf{x}_1', \mathbf{x}_1) \delta \rho_s(\mathbf{x}_2', \mathbf{x}_2)} \phi_b(\mathbf{x}_2) \phi_j^*(\mathbf{x}_2'),\end{aligned}\quad (41)$$

$$O_{ai}^\lambda = \frac{\partial}{\partial \lambda} \left[\int d\mathbf{x} \phi_a^*(\mathbf{x}) \phi_i(\mathbf{x}) \right], \quad (42)$$

$$\left\langle \frac{\partial}{\partial \lambda} a | v_{xc} | i \right\rangle = \int d\mathbf{x} \int d\mathbf{x}' \left[\frac{\partial}{\partial \lambda} \phi_a^*(\mathbf{x}') \right] \frac{\delta E_{xc}}{\delta \rho_s(\mathbf{x}, \mathbf{x}')} \phi_i(\mathbf{x}), \quad (43)$$

$$\begin{aligned} \left(ai | f_{xc} | \frac{\partial}{\partial \lambda} jj \right) &= \int d\mathbf{x}_1 \int d\mathbf{x}'_1 \int d\mathbf{x}_2 \int d\mathbf{x}'_2 \phi_a^*(\mathbf{x}_1) \phi_i(\mathbf{x}'_1) \\ &\quad \times \frac{\delta^2 E_{xc}}{\delta \rho_s(\mathbf{x}'_1, \mathbf{x}_1) \delta \rho_s(\mathbf{x}'_2, \mathbf{x}_2)} \frac{\partial}{\partial \lambda} \left[\phi_j(\mathbf{x}_2) \phi_j^*(\mathbf{x}'_2) \right]. \end{aligned} \quad (44)$$

Now, one can split the excitation energy gradient into two different parts, $\left. \frac{\partial \omega_n}{\partial \lambda} \right|_{\text{direct}}$, which are associated with the explicit derivative with respect to the spatial shift of nuclei positions in the Hamiltonian or the atomic orbitals, and $\left. \frac{\partial \omega_n}{\partial \lambda} \right|_{\text{indirect}}$, which are associated with the molecular orbital coefficient relaxation. After some straightforward but tedious algebra, we arrive at

$$\begin{aligned} \left. \frac{\partial \omega_n}{\partial \lambda} \right|_{\text{direct}} &= - \sum_c \sum_{ab} X_{ab}^n K_{cb} O_{ca}^\lambda - 2 \sum_m \sum_{ab} X_{ab}^n K_{mb} O_{am}^\lambda - \sum_{ab} V_{ab} O_{ab}^\lambda \varepsilon_a \\ &\quad - \sum_{ab} V_{ab} \left[\sum_{nm} O_{nm}^\lambda ((ab|mn) + (ab|f_{xc}|mn)) \right] \\ &\quad + \sum_{a < b, c < d} X_{ab}^n X_{cd}^n \frac{\partial}{\partial \lambda} [(ac|bd) - (ad|bc)] + \sum_{ab} V_{ab} \frac{\partial}{\partial \lambda} \langle a | H^{\text{core}} | b \rangle \\ &\quad + \sum_{ab} V_{ab} \left[\sum_m \frac{\partial}{\partial \lambda} (ab|mm) + \sum_m \left(ab | f_{xc} | \frac{\partial}{\partial \lambda} mm \right) \right] \\ &\quad + \left\langle \frac{\partial}{\partial \lambda} a | v_{xc} | b \right\rangle + \left\langle a | v_{xc} | \frac{\partial}{\partial \lambda} b \right\rangle \\ &\quad - \sum_{ab} \sum_c X_{ab}^n G_{cb} O_{ca}^\lambda + 2 \sum_{ab} \sum_m X_{ab}^n G_{bm} O_{am}^\lambda \\ &\quad - \sum_{hi} \sum_m Y_{hi}^n K_{mi} O_{mh}^\lambda + 2 \sum_{a < b, h < i} X_{ab}^n Y_{hi}^n \frac{\partial}{\partial \lambda} [(ah|bi) - (ai|bh)] \\ &\quad - \sum_{hi} \sum_m Y_{hi}^n G_{mi} O_{mh}^\lambda + \sum_{hi} U_{hi} O_{ih}^\lambda \varepsilon_h \\ &\quad + \sum_{hi} U_{hi} \left[\sum_{nm} O_{nm}^\lambda ((hi|mn) + (hi|f_{xc}|mn)) \right] \\ &\quad + \sum_{h < i, j < k} Y_{hi}^n Y_{jk}^n \frac{\partial}{\partial \lambda} [(hj|ik) - (hk|ij)] \sum_{hi} U_{hi} \frac{\partial}{\partial \lambda} \langle h | H^{\text{core}} | i \rangle \\ &\quad - \sum_{hi} U_{hi} \left[\sum_m \frac{\partial}{\partial \lambda} (hi|mm) + \sum_m \left(hi | f_{xc} | \frac{\partial}{\partial \lambda} mm \right) \right] \\ &\quad + \left\langle \frac{\partial}{\partial \lambda} h | v_{xc} | i \right\rangle + \left\langle h | v_{xc} | \frac{\partial}{\partial \lambda} i \right\rangle, \end{aligned} \quad (45)$$

where the following matrix elements are defined as

$${}^n K_{mb} = \sum_{c < d} X_{cd}^n [(mc|bd) - (md|bc)], \quad (46)$$

$$\begin{aligned} {}^n V_{bc} &= \sum_{(b,c) < d} X_{bd}^n X_{cd}^n + \sum_{d < (b,c)} X_{db}^n X_{dc}^n - \sum_{c < d < b} X_{db}^n X_{cd}^n \\ &\quad - \sum_{b < d < c} X_{bd}^n X_{dc}^n, \end{aligned} \quad (47)$$

$${}^n G_{aj} = \sum_{h < i} Y_{hi}^n [(ah|ji) - (ai|jh)], \quad (48)$$

$${}^n U_{hj} = \sum_{(h,j) < i} Y_{hi}^n Y_{ji}^n + \sum_{i < (h,j)} Y_{ih}^n Y_{ij}^n - \sum_{j < i < h} Y_{ih}^n Y_{ji}^n - \sum_{h < i < j} Y_{hi}^n Y_{ij}^n. \quad (49)$$

And the indirect contribution is given by

$$\left. \frac{\partial \omega_n}{\partial \lambda} \right|_{\text{indirect}} = ({}^n \mathbf{L})^T \mathbf{u}^\lambda = \sum_{am} {}^n L_{am} u_{am}^\lambda, \quad (50)$$

where

$$\begin{aligned} {}^n L_{am} &= -2 \sum_b X_{ab}^n {}^n K_{mb} + 2 \sum_{bc} V_{bc} ((bc|am) + (bc|f_{xc}|am)) \\ &\quad - 2 \sum_i Y_{mi}^n K_{ia} + 2 \sum_b X_{ab}^n G_{bm} \\ &\quad + 2 \sum_j Y_{mj}^n G_{aj} - 2 \sum_{hj} U_{hj} ((hj|am) + (hj|f_{xc}|am)), \end{aligned} \quad (51)$$

Using the Z-vector method⁵⁹ one can calculate the indirect contributions by solving the equation

$$\mathbf{H}^{(1)} \mathbf{z}^n = {}^n \mathbf{L}. \quad (52)$$

and then using the the following relation

$$({}^n \mathbf{L})^T \mathbf{u}^\lambda = (\mathbf{z}^n)^T \mathbf{b}^\lambda. \quad (53)$$

Thus, we have obtained the analytic gradient for the excitation energy contribution of pp-RPA using either HF or DFT reference. Finally, one adds the ground state SCF contribution $\frac{\partial E^{\text{SCF}}}{\partial \lambda}$, for the $N - 2$ electron system or the N -electron system, in Plan A or Plan B, to $\frac{\partial \omega_n}{\partial \lambda}$ to obtain the ground and excited state total energy gradient for the N electron system. An alternative derivation has also been given in the ESI† following the Langrangian approach by Furche and Ahlrichs, which avoids the introduction of the molecular orbital relaxation first derivatives from the very beginning.²¹

III. Computational details

The pp-RPA excitation energy calculations with the HF and DFT references are performed with the QM⁴D quantum chemistry package.⁶⁰ The analytic gradient and geometry optimization are implemented in the QM⁴D quantum chemistry package⁶⁰ for

the HF and the local density approximation (LDA) references in the MO basis for Plan A according to eqn (45), using the

Table 1 Analytic and numerical gradients of the BH molecule for both the ground state $^1\Sigma$ and the doubly excited state $^3\Sigma^-$. The B–H bond length is taken as the ground state experimental value 1.232 Å.⁷⁵ The numerical gradients are calculated by the finite difference method, taking the difference between the energies at 1.233 Å and 1.231 Å. (Unit: Hartree Å⁻¹)

Reference	$\frac{dE(^1\Sigma)}{dR}$	$\frac{dE(^1\Sigma^-)}{dR}$	$\frac{dE(^3\Sigma^-)}{dR}$	$\frac{dE(^3\Sigma^-)}{dR}$
	(analytic)	(numerical)	(analytic)	(numerical)
LDA	-0.02160924	-0.02160884	0.03451664	0.03451460
HF	0.00459937	0.00459903	0.04793338	0.04793303
LDA5050 ^a	-0.01254669	-0.01254751	0.04441725	0.04441517
HF-cLDA ^b	0.00528831	0.00528854	0.05561382	0.05561203

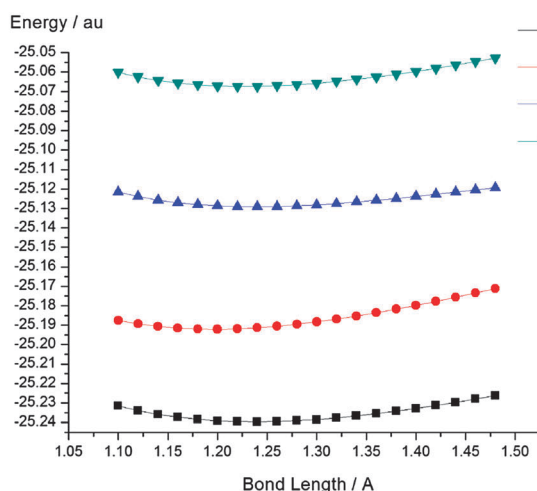
^a LDA5050 stands for $0.5E_x^{\text{HF}} + 0.5E_x^{\text{LDA}} + E_c^{\text{LDA}}$. ^b HF-cLDA stands for $E_x^{\text{HF}} + E_c^{\text{LDA}}$.

Z-vector method.⁵⁹ The B3LYP,^{61,62} CAM-B3LYP,⁶³ CASSCF,⁶⁴ CCSD⁶⁵ and EOM-CCSD^{66,67} calculations are performed with Gaussian 09.⁶⁸ The Full CI and MRCISD(Q)^{69,70} results are obtained with GAMESS.⁷¹ The Cartesian 6-311++G(d,p)^{72–74} basis sets are used.

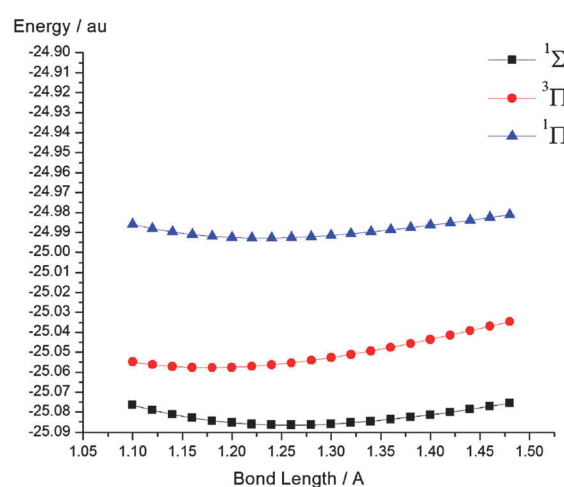
IV. Results and discussion

IV. 1. Verification of analytic and numerical gradient

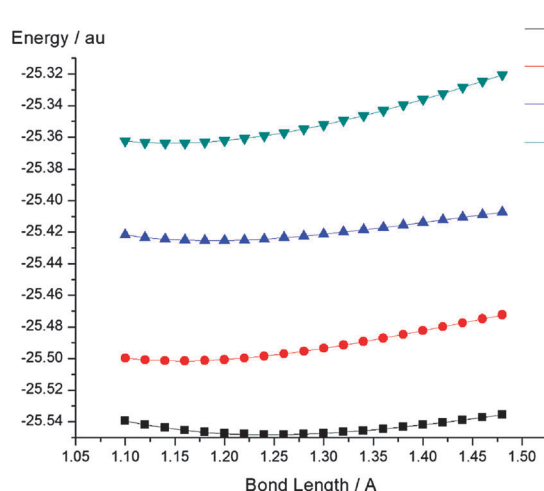
In this section we verify the analytic gradient formula by comparing the analytic and numerical gradient values of the diatomic molecule BH, for both the ground state $^1\Sigma$ and the doubly excited state $^3\Sigma^-$ using Plan A (eqn (27)). According to Table 1, the numerical and analytic gradients for different SCF references are shown to be equivalent, with absolute errors only at the sixth or seventh digit for both the ground state and the doubly excited state.



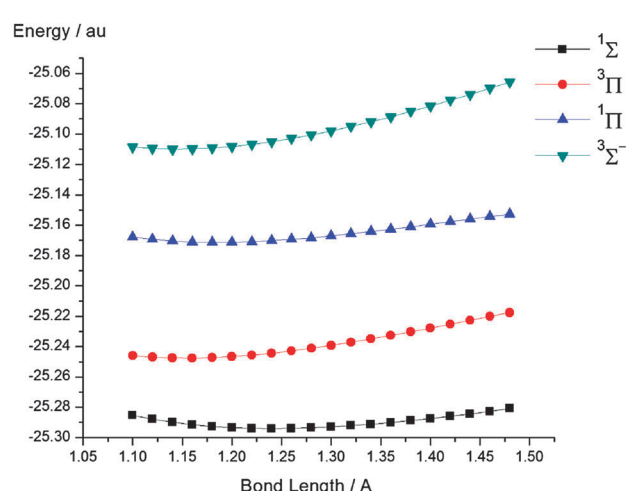
(a) Full CI



(b) (TD-)LDA



(c) Plan A pp-RPA with B3LYP reference



(d) Plan B pp-RPA with B3LYP reference

Fig. 1 Ground and lowest excited state potential energy surfaces of the BH molecule: (a) Full CI; (b) (TD-)LDA; (c) Plan A pp-RPA with B3LYP reference; (d) Plan B pp-RPA with B3LYP reference. The $^3\Sigma^-$ excitation is a HOMO(2)→LUMO(2) double excitation.

Therefore, the analytic gradient formula has been verified to be correct both mathematically and in terms of implementation for both HF and LDA references.

IV. 2. Ground and excited state potential energy surfaces and equilibrium bond lengths of some diatomic molecules

In this section we investigate the ground state and excited state potential energy surfaces with the pp-RPA method. The pp-RPA ground state and excited state total energies of the N -electron systems are calculated from both Plan A and Plan B (see eqn (27) to (28)).

The first two examples are BH and the isoelectric CH^+ . For these two systems the Full CI results are used as benchmark (Fig. 1(a) and 2(a)). The B3LYP reference is adopted for these two systems. The potential energy surfaces for these two systems from both Plan A and Plan B are in agreement with the Full CI curves, with the gaps between different states reasonably well described

(Fig. 1(c), (d), 2(c) and (d)). Particularly, for both systems the reported $^3\Sigma^-$ state is a predominantly doubly excited state from the HOMO σ orbital to the two degenerate LUMO π orbitals, *i.e.* $c|\pi_1\bar{\pi}_2\rangle - c|\pi_2\bar{\pi}_1\rangle$, where c is around 0.69 for BH and 0.68 for CH^+ throughout the bond lengths studied. TDDFT within the adiabatic approximation fails to capture this excitation completely, as is illustrated in the absence of that curve in TD-LDA (Fig. 1(b) and 2(b)), while pp-RPA captures this state correctly. Worse still for TD-LDA in the case of CH^+ , the $^3\Pi$ state is predicted as below the $^1\Sigma$ ground state in energy (Fig. 2(b)). In fact the same is observed for the TD-B3LYP calculation of the BH molecule,²⁸ and such unphysical predictions have been a challenge for the TDDFT description of the lowest triplet excitations. But this issue is qualitatively resolved here within the pp-RPA treatment. Concerning the ground state and excited state bond lengths, the pp-RPA calculations tend to give slightly underestimated results. And the doubly excited state surfaces are less well described,

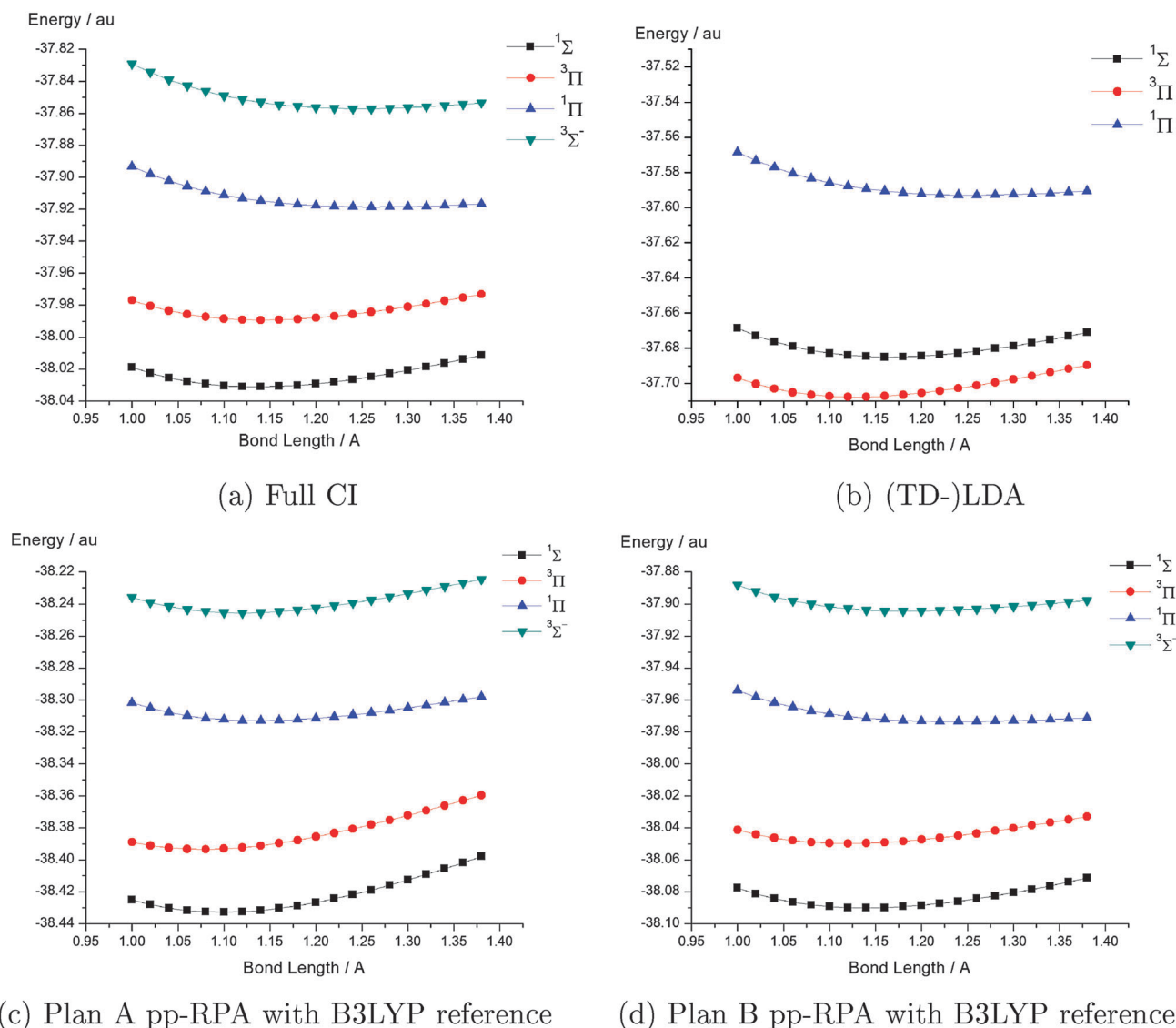


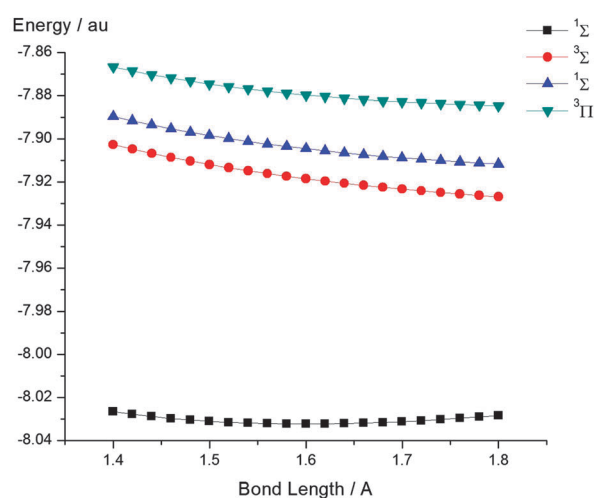
Fig. 2 Ground and lowest excited state potential energy surfaces of the CH^+ molecule: (a) Full CI; (b) (TD-)LDA; (c) Plan A pp-RPA with B3LYP reference; (d) Plan B pp-RPA with B3LYP reference. The $^3\Sigma^-$ excitation is a HOMO(2) \rightarrow LUMO(2) double excitation.

presumably due to the absence of higher excitation contributions. Similarly, predominantly double excitations are also less accurately captured by EOM-CCSD, which is improved only after the triply excited contributions are included, as shown by Table 5 and related comments in ref. 76. A minor improvement is observed when Plan B (28) is used instead of Plan A (27) for CH^+ . The equilibrium bond lengths and adiabatic excitation energies are reported in Tables S1 and S2 in the ESI† for reference.

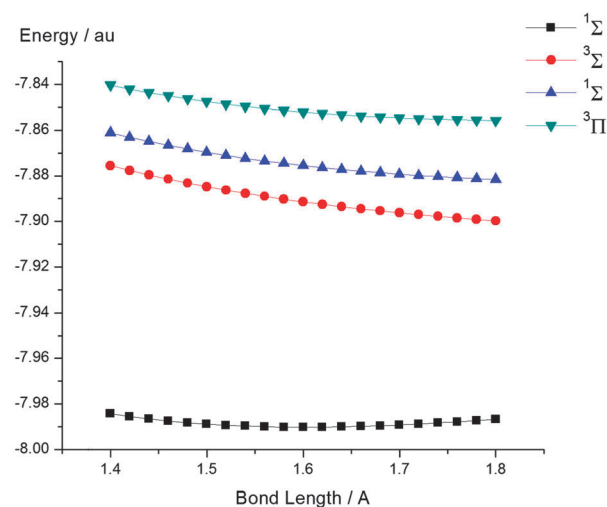
Next, we consider the LiH and NaH molecules around equilibrium bond lengths. For these two systems the (EOM-)CCSD method is chosen as a benchmark, and the HF reference pp-RPA with both Plan A and Plan B is reported here. For the case of LiH, all the methods give reasonable potential energy surfaces, as illustrated in Fig. 3. pp-RPA within both Plan A (27) and Plan B (28) yields slightly better relative energy gaps compared to (TD-)LDA results. The same is true for NaH, as illustrated in Fig. 4, only in

this case the TD-LDA results are clearly worse than those of pp-RPA by widening the gap between the $^3\Sigma$ and $^1\Sigma$ excited state surfaces. However we found that at large bond lengths (TD-)LDA fails qualitatively by greatly overestimating the ground state energy due to its huge static correlation errors. Even EOM-CCSD predicts incorrect energy ordering for the ground state and the lowest triplet excited state. By contrast, pp-RPA accurately reproduces the reference Full CI and MRCISD(Q) results (see ESI† III.3 for detail). Thus it appears that the choice of the $N - 2$ reference system could be critical when significant static correlation is present.

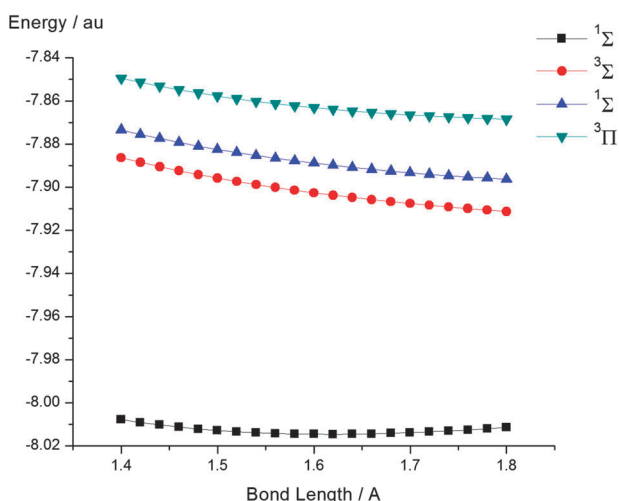
Comparing the two schemes (Plan A and Plan B) for total energy calculations, both schemes calculate the N -particle system excitation energy by taking the difference between two double electron affinities from the $(N - 2)$ -particle SCF reference state, and the calculated N -particle system excitation energy is identical. The difference is only in the choice of the N -particle ground state,



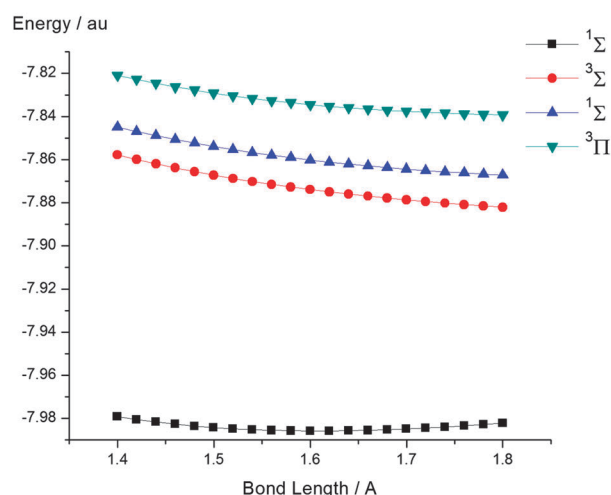
(a) (EOM-)CCSD



(b) (TD-)LDA



(c) Plan A pp-RPA with HF reference



(d) Plan B pp-RPA with HF reference

Fig. 3 Ground and lowest excited state potential energy surfaces of the LiH molecule: (a) (EOM-)CCSD; (b) (TD-)LDA; (c) Plan A pp-RPA with HF reference; (d) Plan B pp-RPA with HF reference.

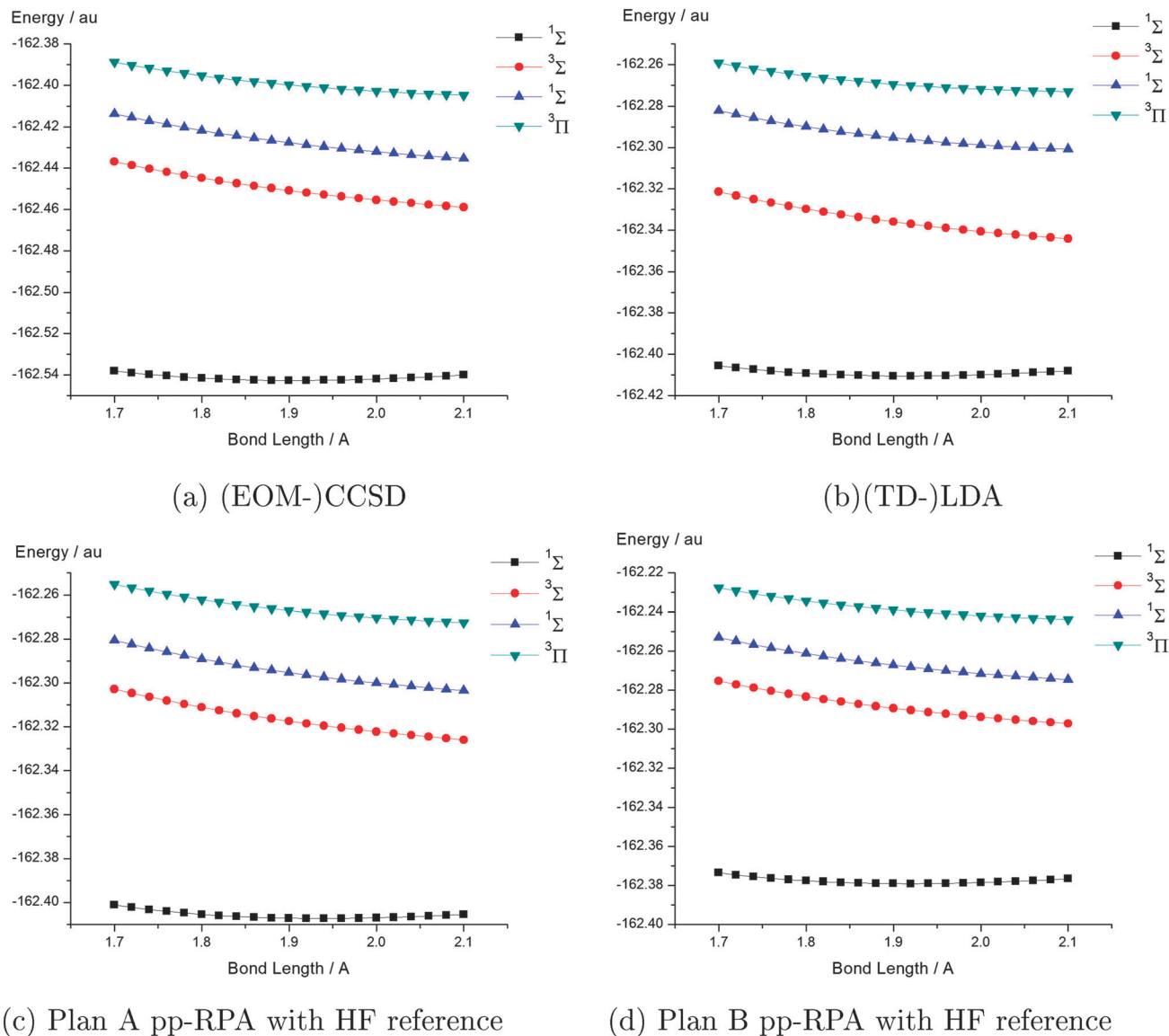


Fig. 4 Ground and lowest excited state potential energy surfaces of the NaH molecule: (a) (EOM-)CCSD; (b) (TD-)LDA; (c) Plan A pp-RPA with HF reference; (d) Plan B pp-RPA with HF reference.

which in Plan B is simply chosen to be the N -particle SCF DFT ground state, while in Plan A it is chosen to be an explicitly correlated double-electron-added state on top of the $(N - 2)$ -particle SCF reference state. The quality of N -particle total energy depends on whether the N -particle DFT ground state or pp-RPA double electron addition ground state is better. The latter explicitly correlates 2 electrons and treats the rest of the $N - 2$ electrons with implicit DFT correlation. Numerically the GS equilibrium geometries are similar for the systems considered. However, for excited state total energy calculations with Plan B, two separate SCF calculations must be performed (one at N and another at $N - 2$). Moreover, although the pp-RPA double electron addition ground state performs similarly as DFT ground state near the equilibrium, the former is superior for stretched single bonds, as will be shown in Section IV. 5 (Fig. 8).

IV. 3. Ground state geometry optimization of some small molecules

In this section we present the optimized ground state structures of some small molecules. Throughout this section Plan A (see eqn (27)) is used to calculate the total energy and the analytic gradient of the ground state. CCSD geometries have been used for benchmarking (Tables 2–4).

The first two examples contain the fluorine element. Specifically, the hypofluorous acid (HFO) (Fig. 5) molecule O–H bond length, as in the case of water, is uniformly underestimated in pp-RPA for all references considered. The LDA reference O–H bond length is in closer proximity to the CCSD benchmark in this case. Also, the O–F bond length is again best captured by the LDA reference. However, in terms of the H–O–F bond angle, pp-RPA results with the HF and LDA references deviate from the CCSD result in opposite directions,

Table 2 Bond lengths and bond angle of HFO

Method	R(H-O)/Å	R(O-F)/Å	A(H-O-F)/deg.
CCSD	0.9670	1.4255	98.63
LDA	0.9822	1.4196	98.78
pp-RPA/HF ref.	0.9029	1.2672	102.19
pp-RPA/HF-cLDA ^a ref.	0.8934	1.2560	102.24
pp-RPA/LDA5050 ^b ref.	0.9115	1.3665	97.79
pp-RPA/LDA ref.	0.9347	1.4399	94.78

^a HF-cLDA stands for $E_x^{\text{HF}} + E_c^{\text{LDA}}$. ^b LDA5050 stands for $0.5E_x^{\text{HF}} + 0.5E_x^{\text{LDA}} + E_c^{\text{LDA}}$.

Table 3 Bond lengths and bond angle of OF₂

Method	R(O-F)/Å	A(F-O-F)/deg.
CCSD	1.3968	103.34
LDA	1.3966	104.63
pp-RPA/HF ref.	1.2500	104.74
pp-RPA/HF-cLDA ^a ref.	1.2393	104.80
pp-RPA/LDA5050 ^b ref.	1.3266	103.14
pp-RPA/LDA ref.	1.3946	103.41

^a HF-cLDA stands for $E_x^{\text{HF}} + E_c^{\text{LDA}}$. ^b LDA5050 stands for $0.5E_x^{\text{HF}} + 0.5E_x^{\text{LDA}} + E_c^{\text{LDA}}$.

Table 4 Bond lengths and bond angle of O₃

Method	R(O-O)/Å	A(O-O-O)/deg.
CCSD	1.2519	117.78
LDA	1.2536	118.61
pp-RPA/HF ref.	1.2353	118.53
pp-RPA/HF-cLDA ^a ref.	1.2199	118.68
pp-RPA/LDA5050 ^b ref.	1.2442	118.11

^a HF-cLDA stands for $E_x^{\text{HF}} + E_c^{\text{LDA}}$. ^b LDA5050 stands for $0.5E_x^{\text{HF}} + 0.5E_x^{\text{LDA}} + E_c^{\text{LDA}}$.

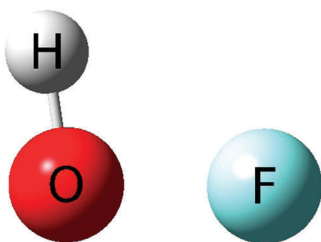


Fig. 5 Structure of the hypofluorous acid molecule.

with the HF and HF-cLDA ($E_x^{\text{HF}} + E_c^{\text{LDA}}$) reference both overestimating the bond angle by about 3.5 degrees and the LDA

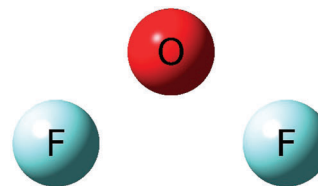


Fig. 6 Structure of the oxygen difluoride molecule.

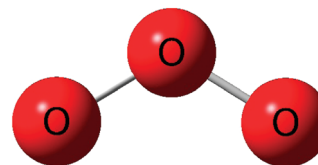


Fig. 7 Structure of the ozone molecule.

reference underestimating it by about 4 degrees. The LDA5050 reference ($0.5E_x^{\text{HF}} + 0.5E_x^{\text{LDA}} + E_c^{\text{LDA}}$) predicts the best bond angle here due to error cancellation (Table 2). Concerning OF₂, both the O-F bond length and the F-O-F bond angle are best captured by the LDA reference pp-RPA, which are very close to the CCSD benchmark results (Fig. 6, Table 3).

The third example presented is the ozone molecule. This molecule has two resonance structures, allowing greater delocalization of electrons throughout the conjugated π bond. For this case, the LDA5050 ($0.5E_x^{\text{HF}} + 0.5E_x^{\text{LDA}} + E_c^{\text{LDA}}$) does best in reproducing both the bond length and bond angle, yielding very similar results compared to CCSD. pp-RPA with the HF-cLDA ($E_x^{\text{HF}} + E_c^{\text{LDA}}$) reference, however, tends to give greater deviation than HF itself in terms of the O-O bond length and the O-O-O bond angle, as is the case in the previous examples considered (Fig. 7, Table 4).

IV. 4. Excited state geometry optimization for water

Now we continue to consider the geometry optimization for the lowest triplet and lowest singlet excitation of the water molecule. The MRCISD(Q) method with 10 active electrons and 7 active orbitals is used for benchmarking. The ground state geometries as well as the total energies of the ground state and excited states are also given for comparison. According to Table 5, we observe that, as for the ground state, there is also a similar underestimation of the O-H bond length in the excited states by pp-RPA in comparison to the benchmark results. The LDA5050 reference

Table 5 Bond lengths and bond angles the ground state, the lowest triple and singlet excited states of the H₂O molecule

Method	¹ A ₁ (ground state)		³ B ₁			¹ B ₁		
	R(O-H)/Å	A(H-O-H)/deg.	R(O-H)/Å	A(H-O-H)/deg.	E. E. ^d /eV	R(O-H)/Å	A(H-O-H)/deg.	E. E. ^d /eV
MRCISD(Q) ^a	0.9612	103.30	1.1122	111.17	6.548	1.0825	105.84	7.058
(TD)LDA	0.9698	105.12	1.0912	108.48	6.010	1.0563	104.18	6.436
pp-RPA/HF ref.	0.9070	108.90	0.9954	104.59	3.127	0.9906	104.22	3.377
pp-RPA/HF-cLDA ^b ref.	0.8969	108.93	0.9934	104.27	3.821	0.9875	103.62	4.105
pp-RPA/LDA5050 ^c ref.	0.9016	107.18	1.0536	102.97	5.596	1.0418	99.27	6.012

^a MRCISD(Q) with 10 active electrons and 7 active orbitals. ^b HF-cLDA stands for $E_x^{\text{HF}} + E_c^{\text{LDA}}$. ^c LDA5050 stands for $0.5E_x^{\text{HF}} + 0.5E_x^{\text{LDA}} + E_c^{\text{LDA}}$.

^d Adiabatic excitation energies.

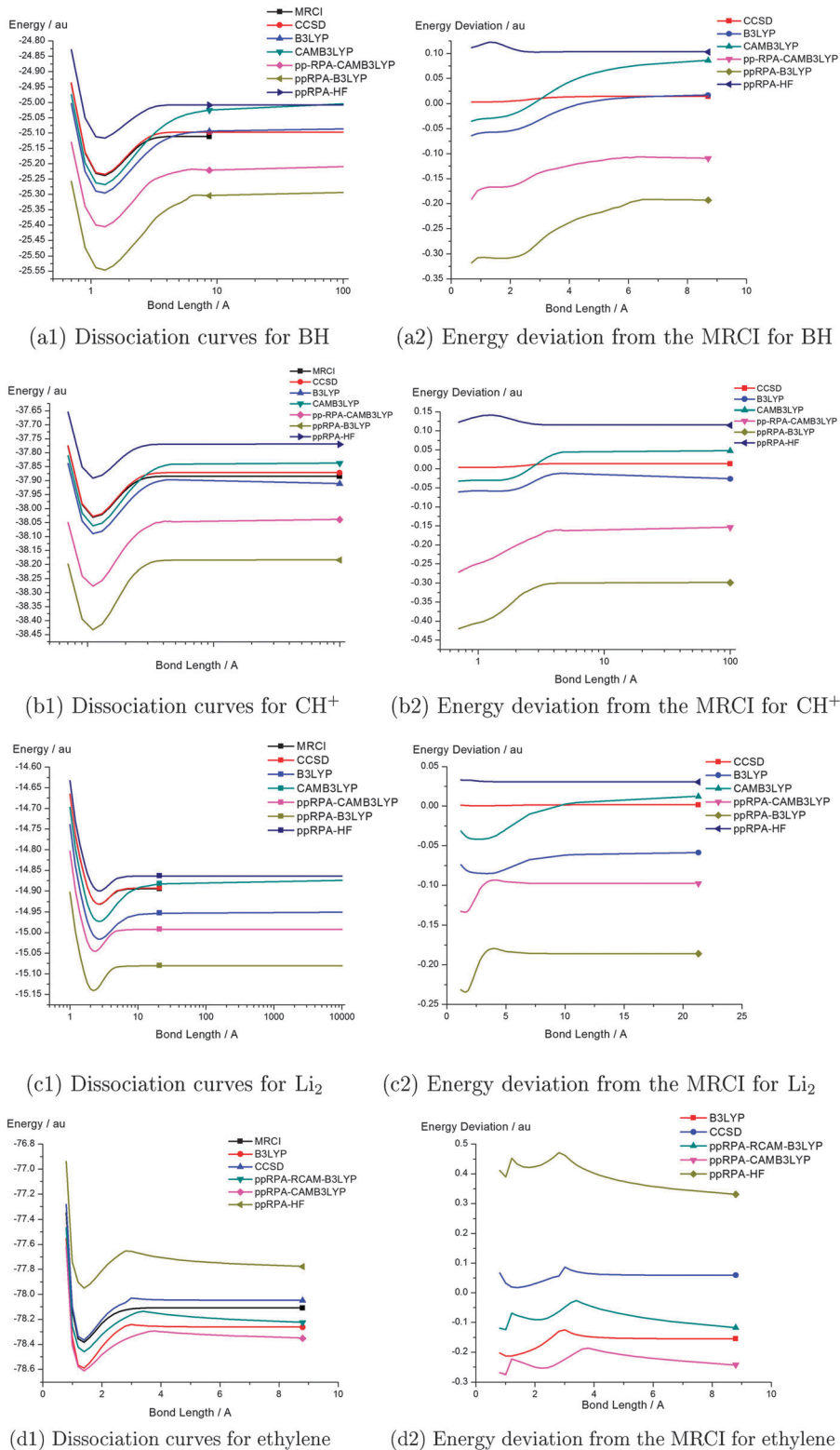


Fig. 8 Bond dissociation curves and energy deviation from the MRCI for BH ((a1) and (a2)); CH⁺ ((b1) and (b2)); Li₂ ((c1) and (c2)); ethylene ((d1) and (d2)). For the dissociation of ethylene we constrain the bond length of C–H to 1.07 Å, and the bond angle of H–C–H to 120 degrees for the C–C bond length scan. The MRCISD(Q) calculations for BH and CH⁺ have 6 active electrons and 6 active orbitals, for Li₂ 6 electrons and 10 orbitals, and for ethylene 12 electrons and 12 orbitals.

$(0.5E_{\text{x}}^{\text{HF}} + 0.5E_{\text{x}}^{\text{LDA}} + E_{\text{c}}^{\text{LDA}})$ performs best of all in terms of both the adiabatic excitation energies and the O–H bond lengths. All methods display the same trend of O–H bond length change

from the ground state 1A_1 to the 3B_1 state and then to the 1B_1 state compared with MRCISD(Q). The improvement of results with increased LDA exchange indicates that DFT references might be

superior for pp-RPA. This superiority of the DFT reference over HF here and in Section IV. 3 indicates the importance of the treatment of the exchange-correlation effect for the $N - 2$ system, in particular when the number of valence electrons is large. For these cases, the LDA reference seems to be an acceptable starting point. We expect the GGA reference to further improve the pp-RPA geometries and plan for further investigation.

IV. 5. Ground state dissociation curves for single and double bonds

In this part we study the ground state dissociation curves for single and double bonds. Throughout this section Plan A (see eqn (27)) is adopted for calculation of the ground state total energy. The CCSD and MRCISD(Q) methods have been used for benchmarking. The MRCISD(Q) calculations for BH and CH⁺ have 6 active electrons and 6 active orbitals, for Li₂ 6 electrons and 10 orbitals, and for ethylene 12 electrons and 12 orbitals.

As far as the single bonds are concerned (see (a1), (a2), (b1), (b2), (c1) and (c2) of Fig. 8), the pp-RPA with the HF reference outperforms that with either the pp-RPA with the B3LYP reference or the CAM-B3LYP reference⁶³ in terms of the shape of the curve and the binding energies, whereas the pp-RPA correlation energy functional from AC-FDT yields unphysical bumps for the potential energy curve of single bond dissociation of H₂ at intermediate bond lengths³⁵ despite its correct dissociating limit. The pp-RPA with the HF reference curves closely resembles those of CCSD and MRCISD(Q), while by contrast the curves obtained with B3LYP, CAM-B3LYP and the pp-RPA calculations with these DFT references all tend to overestimate the binding energy of the molecules. Although pp-RPA with the HF reference gives absolute potential energies that are a little too high, yet we note that this will not be problematic so long as relative energies are concerned. In fact all density functional approximations have deviations in terms of absolute energies (see the B3LYP curve in (c1) of Fig. 8), yet they still prove useful when only relative energies, such as reaction energies, ionization energies, excitation energies, *etc.*, are of interest. Therefore, as long as the energy deviation from the accurate values is reasonably consistent with respect to changing geometries (*e.g.* the pp-RPA curves with the HF reference in (a1), (b1) and (c1)), the method will prove useful in application. For the equilibrium bond lengths as interpolated from cubic splines (Table 6), fairly good agreement is achieved for BH and CH⁺ between the results of pp-RPA with both the HF reference and the B3LYP reference and the results of CCSD and MRCISD(Q). Yet for the case of Li₂, the ground state equilibrium bond lengths predicted by the pp-RPA with the B3LYP and the CAM-B3LYP

references are both severely underestimated, while the pp-RPA with the HF reference gives very accurate result. We ascribe this to the small number of valence electrons (only 2 here), for which the HF orbitals may turn out to be better reference since they make better connection to the configuration interaction picture than DFT orbitals. On the choice of SCF reference, we observe that for relatively small numbers of valence electrons the HF reference gives better results, evidenced by the single-bond dissociation curves in Fig. 8. For larger systems as recently studied with the Davidson's algorithm, B3LYP or other DFT references works better,⁷⁷ also shown in the excited state geometries of water (Tables 4 and 5). Calculations of Rydberg excitations³⁴ shows the HF reference to be better than the B3LYP reference.

However, the situation is trickier with the ethylene molecule. As it is with the pp-RPA correlation energy functional,³⁵ unphysical bumps in the dissociation curves are also observed for intermediate bond lengths for the pp-RPA with both the HF and the CAM-B3LYP references. Also the equilibrium bond lengths are slightly overestimated by pp-RPA with the HF, CAM-B3LYP and rCAM-B3LYP⁷⁸ references. Also we notice that even for CCSD, the dissociation curve is far from satisfactory: the binding energy is a bit too high and the description for intermediate bond lengths is inaccurate. The SCF CAM-B3LYP curve is very similar to that of CCSD, if only it were shifted down by about -0.2 hartrees. To better understand this issue, we remark that the eigenvectors in eqn (1) formally allow for only excitations that add two electrons into the virtual orbitals of the $N - 2$ systems. From a different perspective, if the HF orbitals of the N -electron system are used, known as the HF* scheme, we would obtain something very readily connected to a restricted version of CISD that only accounts for only excitations from HOMO and HOMO $- 1$. Particularly, it has been shown that such a scheme is exact for two-electron systems, like the hydrogen molecule³⁴ (see ESI† for the numerical verification). Therefore, so long as CISD and/or CCSD fails, for instance the dissociation of double or triple bonds, the pp-RPA results will also be problematic, since for such systems the single-determinant reference is already highly questionable. However, as illustrated by the three single-bond dissociation examples, reasonable relative energies can still be obtained so long as the excitations from HOMO and HOMO $- 1$ dominate the configuration space. Also, despite this restriction in configuration space, the recent successful application of pp-RPA to large systems by use of the Davidson's algorithm, featuring single excitation benchmark tests, charge transfer excitations and diradical problems, has obtained very good excitation energies, especially so with DFT references. This, we believe, is a consequence of the inherently built-in correlation by the

Table 6 Interpolated equilibrium bond lengths from the dissociation curves using cubic splines. (Unit: Å)

System	MRCISD(Q)	CCSD	B3LYP	CAM-B3LYP	pp-RPA with different references			
					HF	B3LYP	CAM-B3LYP	rCAM-B3LYP
BH	1.243	1.240	1.237	1.237	1.223	1.250	1.232	—
CH ⁺	1.130	1.130	1.137	1.135	1.115	1.090	1.087	—
Li ₂	2.683	2.682	2.705	2.682	2.700	2.230	2.325	—
Ethylene	1.348	1.354	1.343	—	1.419	—	1.396	1.399

exchange-correlation functionals themselves even for the $N - 2$ reference states.⁷⁷ These exciting results certainly endorse further effort on this unique approach with pp-RPA to tackle electronic excitation problems for sizable molecules of practical interest.

V. Conclusion

The analytic total energy gradient has been developed for excited states calculated from pp-RPA, which is a single-reference counterpart of the DIP/DEA-EOM-CC method. The derivation follows a similar fashion to that of the TDDFT gradient equations. The gradient equations have been verified to be correct *via* a finite difference method for both HF and LDA references. Results with accuracy comparable to DFT/TDDFT have been obtained for ground state and excited potential energies and bond lengths of tested diatomic molecules. Geometry optimization of some small polyatomic molecules also displays a similar accuracy to that of DFT and compares nicely with the benchmark results. Accurate ground state bond dissociation curves are obtained for single bonds, while the results are slightly deteriorated for double bonds. Furthermore, the accuracy of the results depends on a proper choice of the SCF reference for the $(N - 2)$ -particle system. The HF reference works well with small number of valence electrons, while DFT references are better for larger number of valence electrons.

Acknowledgements

D.Z. appreciates the support as part of the Center for the Computational Design of Functional Layered Materials, an Energy Frontier Research Center funded by the U.S. Department of Energy, Office of Science, Basic Energy Sciences under Award # DE-SC0012575. D.Z. also acknowledges the support of the Joe Taylor Adams Fellowship from Duke University. W.Y. appreciates the support from National Science Foundation (CHE-1362927).

References

- M. R. Wasielewski, *Chem. Rev.*, 1992, **92**, 435.
- J. H. Alstrum-Acevedo, M. K. Brennaman and T. J. Meyer, *Inorg. Chem.*, 2005, **44**, 6802.
- C. J. Gagliardi, B. C. Westlake, C. A. Kent, J. J. Paul, J. M. Papanikolas and T. J. Meyer, *Coord. Chem. Rev.*, 2010, **254**, 2459.
- J. B. Foresman, M. Head-Gordon, J. A. Pople and M. J. Frisch, *J. Phys. Chem.*, 1992, **96**, 135.
- M. Head-Gordon, R. J. Rico, M. Oumi and T. J. Lee, *Chem. Phys. Lett.*, 1994, **219**, 21.
- M. Head-Gordon, D. Maurice and M. Oumi, *Chem. Phys. Lett.*, 1995, **246**, 114.
- I. Shavitt, in *Methods in Electronic Structure*, ed. H. F. Schaeffer III, 1977, pp. 462–490.
- F. Neese, T. Petrenko, D. Ganyushin and G. Olbrich, *Coord. Chem. Rev.*, 2007, **251**, 288.
- B. O. Roos, P. Linse, P. E. Siegbahn and M. R. Blomberg, *Chem. Phys.*, 1982, **66**, 197.
- K. Wolinski, H. L. Sellers and P. Pulay, *Chem. Phys. Lett.*, 1987, **140**, 225.
- B. O. Roos, K. Andersson, M. P. Fulscher, L. Serrano-Andres, K. Pierloot, M. Merchon and V. Molina, *J. Mol. Struct.: THEOCHEM*, 1996, **388**, 257.
- H. Sekino and R. J. Bartlett, *Int. J. Quantum Chem.*, 1984, **26**, 255.
- J. F. Stanton and R. J. Bartlett, *J. Chem. Phys.*, 1993, **98**, 7029.
- K. Kowalski and P. Piecuch, *J. Chem. Phys.*, 2000, **113**, 8490.
- A. I. Krylov, *Annu. Rev. Phys. Chem.*, 2008, **59**, 433.
- P. Hohenberg and W. Kohn, *Phys. Rev.*, 1964, **136**, B864.
- W. Kohn and L. J. Sham, *Phys. Rev.*, 1965, **140**, A1133.
- A. J. Cohen, P. Mori-Sánchez and W. Yang, *Chem. Rev.*, 2011, **112**, 289.
- E. Runge and E. K. Gross, *Phys. Rev. Lett.*, 1984, **52**, 997.
- M. Casida, in *Recent Advances in Density Functional Methods Part A*, ed. P. D. Chong, 1995, pp. 155–192.
- F. Furche and R. Ahlrichs, *J. Chem. Phys.*, 2002, **117**, 7433.
- E. Salpeter and H. Bethe, *Phys. Rev.*, 1951, **84**, 1232.
- L. Hedin, *Phys. Rev.*, 1965, **139**, A796.
- L. Sham and T. Rice, *Phys. Rev.*, 1966, **144**, 708.
- M. S. Hybertsen and S. G. Louie, *Phys. Rev. B: Condens. Matter Mater. Phys.*, 1986, **34**, 5390.
- R. Godby, M. Schlüter and L. Sham, *Phys. Rev. B: Condens. Matter Mater. Phys.*, 1988, **37**, 10159.
- A. Marini and R. Del Sole, *Phys. Rev. Lett.*, 2003, **91**, 176402.
- D. Zhang, S. N. Steinmann and W. Yang, *J. Chem. Phys.*, 2013, **139**, 154109.
- J. F. Dobson, M. J. Bünner and E. K. U. Gross, *Phys. Rev. Lett.*, 1997, **79**, 1905.
- N. T. Maitra, F. Zhang, R. J. Cave and K. Burke, *J. Chem. Phys.*, 2004, **120**, 5932.
- M. E. Casida, *J. Chem. Phys.*, 2005, **122**, 054111.
- M. Gatti, V. Olevano, L. Reining and I. V. Tokatly, *Phys. Rev. Lett.*, 2007, **99**, 057401.
- W. Dickhoff and D. Van Neck, *Many-Body Theory Exposed - Propagator Description of Quantum Mechanics in Many-Body Systems*, World Scientific Publishing Co. Pte. Ltd, 2005, pp. 185–186.
- Y. Yang, H. van Aggelen and W. Yang, *J. Chem. Phys.*, 2013, **139**, 224105.
- H. van Aggelen, Y. Yang and W. Yang, *Phys. Rev. A*, 2013, **88**, 030501(R).
- P. Mori-Sánchez, A. J. Cohen and W. Yang, *Phys. Rev. Lett.*, 2009, **102**, 066403.
- Y. Yang, H. van Aggelen, S. N. Steinmann, D. Peng and W. Yang, *J. Chem. Phys.*, 2013, **139**, 174110.
- D. Peng, S. N. Steinmann, H. van Aggelen and W. Yang, *J. Chem. Phys.*, 2013, **139**, 104112.
- G. E. Scuseria, T. M. Henderson and I. W. Bulik, *J. Chem. Phys.*, 2013, **139**, 104113.
- J. Gerratt and I. M. Mills, *J. Chem. Phys.*, 1968, **49**, 1719.
- C. Van Caillie and R. D. Amos, *Chem. Phys. Lett.*, 1999, **308**, 249.

- 42 C. Van Caillie and R. D. Amos, *Chem. Phys. Lett.*, 2000, **317**, 159.
- 43 D. Rappoport and F. Furche, *J. Chem. Phys.*, 2007, **126**, 201104.
- 44 J. Liu and W. Liang, *J. Chem. Phys.*, 2011, **135**, 184111.
- 45 J. F. Stanton and J. Gauss, *J. Chem. Phys.*, 1994, **101**, 8938.
- 46 H. Lischka, M. Dallos and R. Shepard, *Mol. Phys.*, 2002, **100**, 1647.
- 47 C. S. Page and M. Olivucci, *J. Comput. Chem.*, 2003, **24**, 298.
- 48 M. Ben-Nun and T. J. Martinez, *Adv. Chem. Phys.*, 2002, **121**, 439.
- 49 D. Peng and W. Yang, *J. Chem. Phys.*, 2013, **138**, 184108.
- 50 L. Oliveira, E. Gross and W. Kohn, *Phys. Rev. Lett.*, 1988, **60**, 2430.
- 51 Y. Shao, M. Head-Gordon and A. I. Krylov, *J. Chem. Phys.*, 2003, **118**, 4807.
- 52 F. Wang and T. Ziegler, *J. Chem. Phys.*, 2004, **121**, 12191.
- 53 M. Seth, G. Mazur and T. Ziegler, *Theor. Chem. Acc.*, 2011, **129**, 331.
- 54 Y. A. Bernard, Y. Shao and A. I. Krylov, *J. Chem. Phys.*, 2012, **136**, 204103.
- 55 M. Nooijen and R. J. Bartlett, *J. Chem. Phys.*, 1997, **107**, 6812.
- 56 K. W. Sattelmeyer, H. F. Schaefer III and J. F. Stanton, *Chem. Phys. Lett.*, 2003, **378**, 42.
- 57 J. Shen and P. Piecuch, *J. Chem. Phys.*, 2013, **138**, 194102.
- 58 D. Peng, H. van Aggelen, Y. Yang and W. Yang, *J. Chem. Phys.*, 2014, **140**, 18A522.
- 59 N. C. Handy and H. F. Schaefer III, *J. Chem. Phys.*, 1984, **81**, 5031.
- 60 QM4D, An in-house program for QM-MM simulation, see <http://www.qm4d.info>.
- 61 C. Lee, W. Yang and R. G. Parr, *Phys. Rev. B: Condens. Matter Mater. Phys.*, 1988, **37**, 785.
- 62 A. D. Becke, *J. Chem. Phys.*, 1993, **98**, 5648.
- 63 T. Yanai, D. P. Tew and N. C. Handy, *Chem. Phys. Lett.*, 2004, **393**, 51.
- 64 D. Hegarty and M. A. Robb, *Mol. Phys.*, 1979, **38**, 1795.
- 65 I. Shavitt, in *Methods in Electronic Structure*, ed. H. F. Schaeffer III, 1977, pp. 299–308.
- 66 J. Geertsen, M. Rittby and R. J. Bartlett, *Chem. Phys. Lett.*, 1989, **164**, 57.
- 67 D. C. Comeau and R. J. Bartlett, *Chem. Phys. Lett.*, 1993, **207**, 414.
- 68 M. J. Frisch, G. W. Trucks, H. B. Schlegel, G. E. Scuseria, M. A. Robb, J. R. Cheeseman, G. Scalmani, V. Barone, B. Mennucci, G. A. Petersson, H. Nakatsuji, M. Caricato, X. Li, H. P. Hratchian, A. F. Izmaylov, J. Bloino, G. Zheng, J. L. Sonnenberg, M. Hada, M. Ehara, K. Toyota, R. Fukuda, J. Hasegawa, M. Ishida, T. Nakajima, Y. Honda, O. Kitao, H. Nakai, T. Vreven, J. A. Montgomery, Jr., J. E. Peralta, F. Ogliaro, M. Bearpark, J. J. Heyd, E. Brothers, K. N. Kudin, V. N. Staroverov, R. Kobayashi, J. Normand, K. Raghavachari, A. Rendell, J. C. Burant, S. S. Iyengar, J. Tomasi, M. Cossi, N. Rega, J. M. Millam, M. Klene, J. E. Knox, J. B. Cross, V. Bakken, C. Adamo, J. Jaramillo, R. Gomperts, R. E. Stratmann, O. Yazyev, A. J. Austin, R. Cammi, C. Pomelli, J. W. Ochterski, R. L. Martin, K. Morokuma, V. G. Zakrzewski, G. A. Voth, P. Salvador, J. J. Dannenberg, S. Dapprich, A. D. Daniels, O. Farkas, J. B. Foresman, J. V. Ortiz, J. Cioslowski and D. J. Fox, *Gaussian 09, Revision A.02*, Gaussian, Inc., Wallingford CT, 2009.
- 69 S. R. Langhoff and E. R. Davidson, *Int. J. Quantum Chem.*, 1974, **8**, 61.
- 70 P. J. Bruna, S. D. Peyerimhoff and R. J. Buenker, *Chem. Phys. Lett.*, 1980, **72**, 278.
- 71 M. W. Schmidt, K. K. Baldrige, J. A. Boatz, S. T. Elbert, M. S. Gordon, J. H. Jensen, S. Koseki, N. Matsunaga, K. A. Nguyen, S. Su, T. L. Windus, M. Dupuis and J. A. Montgomery Jr., *J. Comput. Chem.*, 1993, **14**, 1347.
- 72 W. J. Hehre, R. Ditchfield and J. A. Pople, *J. Chem. Phys.*, 1972, **56**, 2257.
- 73 J. D. Dill and J. A. Pople, *J. Chem. Phys.*, 1975, **62**, 2921.
- 74 C. Hariharan, *J. Chem. Phys.*, 1982, **77**, 3654.
- 75 K. P. Huber and G. Herzberg, *Molecular spectra and nmolecular structure, Vol. IV. Constants of diatomic molecules*, Van Nostrand Reinhold, New York, 1979.
- 76 R. J. Bartlett and M. Musiał, *Rev. Mod. Phys.*, 2007, **79**, 291.
- 77 Y. Yang, D. Peng, J. Lu and W. Yang, *J. Chem. Phys.*, 2014, **141**, 124104.
- 78 A. J. Cohen, P. Mori-Sanchez and W. Yang, *J. Chem. Phys.*, 2007, **126**, 191109.